

Rotational magnetic particles microrheology: The Maxwellian caseC. Wilhelm,¹ J. Browaeys,² A. Ponton,² and J.-C. Bacri¹¹*Fédération de Recherche, FR2438 Matière et Systèmes Complexes and Laboratoire des Milieux Désordonnés et Hétérogènes, Université Paris 6, Case 78, 4 Place Jussieu, 75252 Paris Cedex 05, France*²*Fédération de Recherche, FR2438 Matière et Systèmes Complexes and Laboratoire de Biorhéologie et d'Hydrodynamique Physico Chimique, Université Paris 7, Case 7056, 2 Place Jussieu, 75251 Paris Cedex 05, France*

(Received 12 June 2002; published 22 January 2003)

An experimental method based on the rotational dynamics of a magnetic probe is reported to measure the local viscoelasticity of soft materials on microscopic scales. The technique is based on the alignment of dipolar chains of submicrometer magnetic particles in the direction of an applied magnetic field. On one hand, light scattering is used to detect the chains' oscillations over a 0.001–100 Hz frequency range when submitted to an oscillating magnetic field and leads to global microrheological measurements. On the other hand, the chains' rotation toward a permanent magnetic field is observed with a microscope, allowing a local determination of viscoelastic properties on the scale of the chains of particles. We demonstrate the accuracy of both assays with a micellar Maxwellian solution and validate theoretical predictions.

DOI: 10.1103/PhysRevE.67.011504

PACS number(s): 83.85.Cg, 83.60.Bc, 75.50.Mm, 82.70.Dd

I. INTRODUCTION

Microrheology is a promising technique to measure viscoelastic properties of soft materials that cannot be produced in bulk quantities (from biological polymers to living cells) or to probe the local viscoelastic behavior of rheologically inhomogeneous materials. This has led, during the last decade, to more and more studies focusing on probing complex fluids on microscopic scales. All techniques that are presently used consist in measuring the response of embedded colloidal spherical particles (typical diameter in the range of a few micrometers) to external forces. These microrheological methods, using small probe particles, fall into two categories. The first involves an active manipulation of the probes within the sample: a controlled force is exerted on the particles via either external magnetic fields [1–3] or laser tweezers [4]. The second uses particles as passive probes within the material: the thermally fluctuating positions of the particles undergoing Brownian motion are observed and the viscoelasticity is deduced using the fluctuation dissipation theorem [5–8,11]. The local measurements obtained by these microrheological techniques often differ from macroscopic measurements [12,13], possibly due to the interactions of the particle size with the different scales of the probed material [14]. Both techniques involve the translational movements of a spherical probe of characteristic diameter d . The magnetic and optical forces vary as d^3 and the Brownian forces as $k_B T/d$. These forces are compensated by the fluid friction which varies as d . This difference makes it difficult to analyze the size dependence of the rheological behavior. Recent work [15] extended translational thermally driven diffusion microrheology to the study of the rotational diffusion of anisotropically shaped particles, opening the field of rotational microrheology measurements. As the rotational dynamics is thermally induced, the problem of size dependencies still holds. In contrast, if one considers an active probe submitted to an external magnetic torque, the angular rotation of the probe is independent of its size: the viscoelastic friction torque is proportional to d^3 , as for the magnetic torque. Ro-

tating probes should therefore become more effective in exploring the viscoelastic properties of soft materials and their scaling. Precise knowledge of the probe diameter, which is often a problem for micrometer-sized particles, is no longer an issue. The dynamics of pairs of magnetic holes [16] or chains of magnetic particles [17] submitted to a rotating magnetic field have been fully characterized in viscous fluids. The rotation of a single micrometer-sized particle was also used to study the microrheology of Newtonian fluids [18], with magnetic detection. As far as we know, viscoelastic properties of soft materials have not been explored yet using active manipulation of rotating probes. In this paper, we propose a technique of microrheology based on either the oscillation of chains of micrometer-sized magnetic particles or their rotation toward the direction of a permanent magnetic field. The theoretical principles are described first, and then the technique is tested and validated by probing the microrheology of solutions exhibiting Maxwellian linear viscoelastic behavior.

II. THEORY**A. Maxwell rheological model for a rotating geometry**

Our aim is to apply the well known Maxwell viscoelastic model to a rotating geometry. As illustrated in Figs. 1(a) and 1(b), the Maxwell mechanical equivalent circuit of a spring and a dashpot in series consists of a dashpot coupled to a torsion wire. The displacement z of a particle in translation is linked to the applied force F according to

$$\frac{dz}{dt} = \frac{1}{k} \frac{dF}{dt} + \frac{F}{\xi}, \quad (1)$$

where k is the spring elastic constant and ξ the dashpot viscous constant, these constants being proportional, respectively, to the Young modulus and viscosity with a factor depending on the geometry of the particle. We transpose this equation to describe the rotation of a particle inside a Maxwellian fluid and submitted to an applied torque Γ , writing

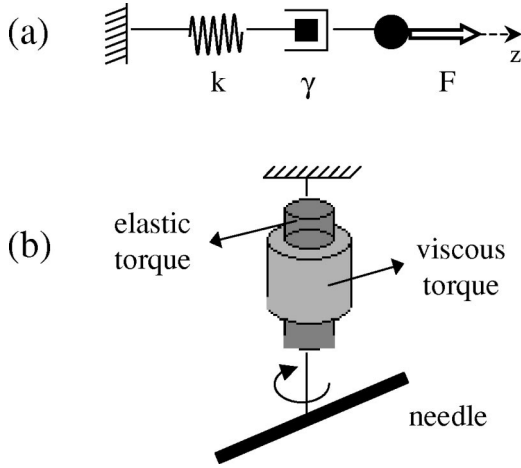


FIG. 1. (a) Maxwell mechanical equivalent circuit describing the displacement of a translating probe submitted to an external magnetic force and (b) equivalent for a rotating probe submitted to an external magnetic torque: a torsion wire (elastic constant C) is then connected to a dashpot (viscous constant γ).

the angular velocity as the sum of an elastic contribution (elastic torque $C\theta$) and a dissipative contribution (friction torque $\gamma\dot{\theta}$):

$$\frac{d\theta}{dt} = \frac{1}{C} \frac{d\Gamma}{dt} + \frac{\Gamma}{\gamma}, \quad (2)$$

where C and γ are, respectively, the elastic and viscous constants. This equivalence has previously been verified [19] by comparing the analysis of the translation of a macroscopic (1 mm diameter) magnetic bead inside a Maxwellian fluid to the analysis of the rotation of a macroscopic (0.05 mm diameter, 0.5 mm length) magnetic needle inside the same fluid.

B. Viscoelastic torques

The elastic and dissipative rotational constants C and γ are directly related to the shear modulus G and viscosity η by elastic and dissipative geometrical factors, respectively, κ_e and κ_d :

$$C = \kappa_e V G \quad \text{and} \quad \gamma = \kappa_d V \eta, \quad (3)$$

where V is the volume of the rotating object. For a spherical particle of diameter d rotating in a medium of viscosity η , the expression for the dissipative torque [20], $\Gamma_d = -\pi d^3 \eta d\theta/dt$ (d is the particle diameter), directly gives $\kappa_d = 6$. It has been recently demonstrated [21] that, in the case of the rotation of a spherical particle in a homogeneous elastic medium, the elastic torque exerted on the bead is written as $\Gamma_e = -\pi d^3 G \theta$, so that $\kappa_e = \kappa_d = 6$. Note that this equality can also be explained by considering the generalized Stokes-Einstein relation (see [8] for instance). For a chain of N spherical particles, the dissipative constant κ_d has been calculated using the Shish-Kebab model [9], with N large compared to unity (see Fig. 2):

$$\kappa_d(N) = \frac{2N^2}{\ln(N/2)}. \quad (4)$$

For chains containing less than ten particles, a more precise estimation of κ_d can be obtained by assimilating the chain of particles to a prolate ellipsoid (with an aspect ratio equal to N) [10]. We suggest a simple phenomenological function that describes κ_d , in our experiment, for any size of chain:

$$\kappa_d(N) = \frac{2N^2}{\ln(N/2) + b/N}. \quad (5)$$

The value of b is determined by fitting experimental data using Eq. (5) (see Sec. IV B): $b = 2.4$. The geometrical elastic rotation factor κ_e has not yet been calculated for an ellipsoidal shape. Let us assume that, as found for a sphere, $\kappa_e = \kappa_d = \kappa$ for chains of particles. This hypothesis will be experimentally confirmed further (see Secs. IV and V).

C. Magnetic torque and mechanical equilibrium

The particles used in this study exhibit a paramagneticlike behavior: an external magnetic field \vec{H} induces a magnetic dipolar moment $\vec{m} = (\pi/6)d^3\chi\vec{H}$, where $\chi = M/H$ is the magnetic susceptibility at the corresponding field, M the magnetization, and d the particles diameter. The magnetic torque applied to a chain of N particles was calculated in [17]. Briefly, one must sum all the torques that are exerted on each particle due to the magnetic interaction of the particle with its near neighbors. Each chain is finally submitted to the magnetic torque

$$\Gamma = \frac{3\mu_0 m^2}{4\pi} \frac{N^2}{2d^3} \sin[2(\beta - \theta)] = \kappa_m V \frac{\sin[2(\beta - \theta)]}{2}, \quad (6)$$

where $V = N(\pi/6)d^3$ is the chain volume and using the angle notations of Fig. 2(a). The magnetic factor κ_m expressed in Pa can be simply rewritten as

$$\kappa_m(N, H) = \frac{\mu_0}{8} N \chi^2 H^2. \quad (7)$$

Equation (2) then becomes

$$K \frac{d\theta}{dt} = \frac{1}{2G} \frac{d}{dt} \{ \sin[2(\beta - \theta)] \} + \frac{1}{2\eta} \sin[2(\beta - \theta)], \quad (8)$$

where G and η are, respectively, the shear modulus and the viscosity of the surrounded material and

$$K(N, H) = \frac{\kappa}{\kappa_m}. \quad (9)$$

K is in Pa^{-1} and can be viewed as the inverse of an equivalent magnetic shear modulus. As mentioned in the Introduction, as K only depends upon the number of particles within the chain, the chain dynamic does not vary with the particle size.

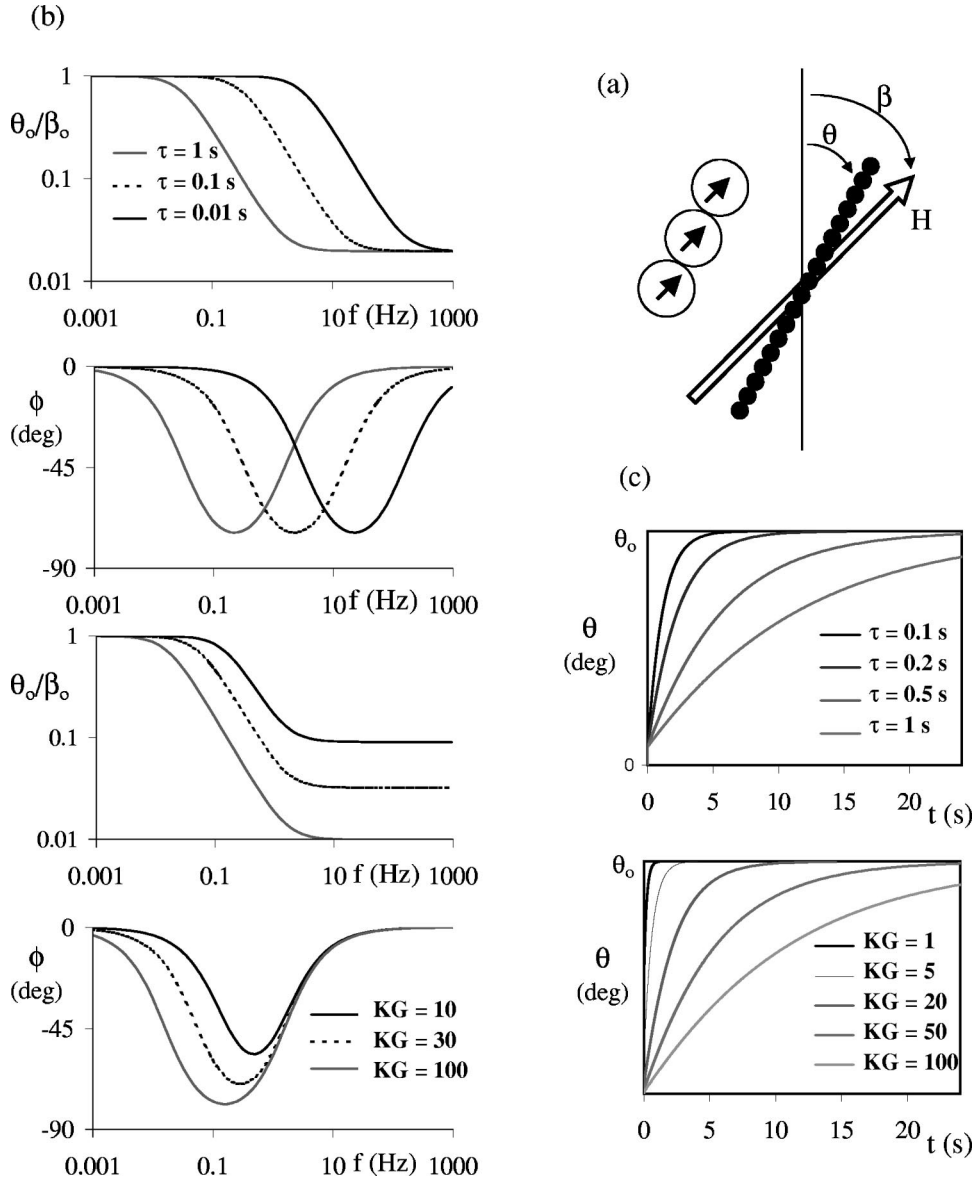


FIG. 2. (a) The rotating probe consists of a chain of N paramagnetic spherical particles. θ is the angle from the initial needle position and $(\beta - \theta)$ the angle between the needle and the applied magnetic field. Each magnetic moment μ of the particles within the chain is oriented along the field (paramagnetic behavior). (b) Theoretical Bode diagram of the angular response (amplitude and phase) of chains of magnetic particles dispersed in a Maxwellian fluid submitted to a spatially oscillating magnetic field. The dependence on relaxation time τ (for a given $KG = 50$) is illustrated above and the effect of parameter KG (for a given $\tau = 0.1$ s) is shown below. (c) The theoretical angle response of a magnetic particle chain, submitted to a magnetic field initially at angle $\beta_0 = 25^\circ$. The effects of variation of the relaxation time τ ($KG = 50$) and of the parameter KG ($\tau = 0.1$ s) are illustrated, respectively, above and below.

Using Eq. (8), the shear modulus and the viscosity of the fluid under investigation are measured via the analysis of the motion of the chain in response to either an oscillating magnetic field or a step magnetic field.

D. Oscillating chains

Let us first consider a perturbation consisting of a magnetic field \vec{H} whose direction oscillates within the angles $[-\beta_0; \beta_0]$ at frequency ω : the field angle β is written as $\beta = \beta_0 \sin(\omega t)$. The chains of particles then oscillate within the angles $[-\theta_0; \theta_0]$, with a phase lag φ : $\theta = \theta_0 \sin(\omega t + \varphi)$. Using complex notation, $\beta = \beta_0 e^{i\omega t}$ and $\theta = \theta_0 e^{i(\omega t + \varphi)}$, Eq. (8) directly gives, for $\beta_0 \ll 1$,

$$\theta_0 = \beta_0 \frac{1 + i\omega\tau}{1 + i\omega\tau(1 + KG)}, \quad (10)$$

where

$$\tau = \frac{\eta}{G} \quad (11)$$

is the viscoelastic relaxation time.

The phase and magnitude are easily deduced:

$$\frac{\theta_0}{\beta_0} = \frac{1}{\sqrt{[1 + (\omega\tau)^2] \{1 + [\omega\tau(1 + KG)]^2\}}}, \quad (12)$$

$$\varphi = \{\arctan(\omega\tau) - \arctan[(1 + KG)\omega\tau]\}, \quad (13)$$

and are represented in Fig. 2(b) for different relaxation times and constants K . The frequency ω_m and value $\varphi(\omega_m)$ of the phase minimum,

$$\omega_m = \frac{1}{\tau} \sqrt{1/(1 + KG)}, \quad \varphi(\omega_m) = \frac{\pi}{2} - 2 \arctan \sqrt{1 + KG}, \quad (14)$$

allow a direct determination of τ and G (assuming that K is known).

E. Rotation toward a permanent magnetic field

We now model the dynamic of the chains when a permanent homogeneous magnetic field H is switched on at $t=0$ in a direction that makes an angle β_0 with the chains. Angle notations are given in Fig. 2(a) and the motion of a chain toward \vec{H} is governed by Eq. (8) with $\beta=\beta_0$. An analytical solution for $t(\theta)$ exists, for any β_0 :

$$t = \tau \left\{ \ln \frac{\sin[2(\beta_0 - \theta_0)]}{\sin[2(\beta_0 - \theta)]} + KG \ln \frac{\tan(\beta_0 - \theta_0)}{\tan(\beta_0 - \theta)} \right\}$$

$$\text{with } 2\theta_0 = \frac{\sin[2(\beta_0 - \theta_0)]}{KG}. \quad (15)$$

The typical response curves are shown in Fig. 2(c) for different sets of parameters. The viscosity η governs the long-time rotation toward the field. The instantaneous angle jump at $t=0$ directly gives G : the higher G , the smaller the jump.

III. MATERIALS AND METHODS

A. Magnetic beads

Superparamagnetic particles of 650 nm hydrodynamic diameter made of maghemite nanoparticles (volume fraction 3.4%) dispersed in low density polystyrene (Merck, Estapor, M1030/40) were used to probe soft materials on microscopic scales. To measure their magnetization, the particles are suspended in gel at known volumic concentration and are oscillated in the same direction as a magnetic field created by an electromagnet. The corresponding emf generated in detection coils is measured at the oscillation frequency. One obtains (Fig. 3) the magnetization curve $M_v(H)$ for the magnetic bead, illustrating the paramagneticlike behavior of the particles. The magnetic susceptibility of the particles was $\chi = 0.07$ for $B = 0.2$ T ($H = 160$ kA m⁻¹) and 0.12 for $B = 0.1$ T ($H = 80$ kA m⁻¹), which are the two magnetic field amplitudes used in this study. The volume concentration of the particles in all the samples used in the experiments was $\phi = 5 \times 10^{-4}$.

B. Micellar solutions

Solutions of surfactant molecules in aqueous solutions were chosen for this study due to their linear viscoelastic properties following the Maxwell model. The cationic surfactant cethyltrimethylammonium chloride (CTAC) forms cylindrical micelles which entangle and confer viscoelastic properties on the fluid. CTAC is diluted in distilled water at [CTAC]=0.1M with an additive salt [NaSal]=0.12M. The solution of micelles obtained was mechanically characterized using a Couette rheometer for five different temperatures: 25, 27.5, 30, 32.5, and 35 °C. Figure 4(a), representing G'' as a function of G' , illustrates the Maxwell behavior of the solution: the semicircle observed on this Cole-Cole plot reflects the following frequency dependence for G' and G'' :

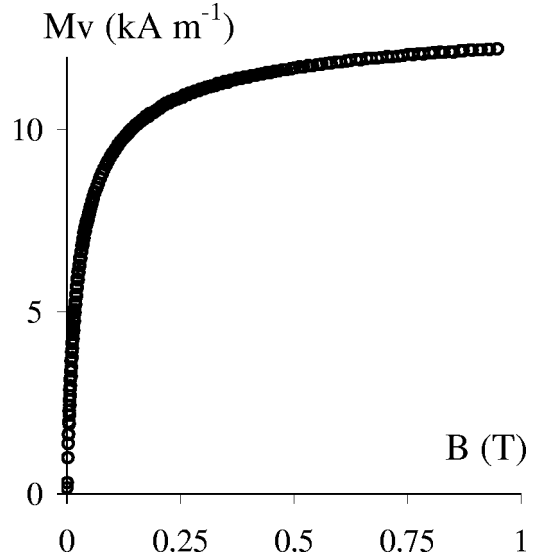


FIG. 3. Magnetization M_v of a magnetic particle as a function of the applied field. The particles are paramagnetic: magnetization increases with the field and, when the field decreases, there is no remanent magnetization.

$$G' = \frac{G\omega^2\tau_R^2}{1 + \omega^2\tau_R^2} \quad \text{and} \quad G'' = \frac{G\omega\tau_R}{1 + \omega^2\tau_R^2}. \quad (16)$$

G is the shear modulus and $\tau_R = \eta/G$ the viscoelastic relaxation time, measured in a classical rheology experiment. For the micellar solution under consideration, the shear modulus G is almost independent of temperature, whereas the relaxation time drastically decreases with increasing temperature. Figure 4(b) shows the temperature dependence of both shear modulus G and viscosity η .

C. Light scattering

Chains are first formed within the sample in a 0.2 T magnetic field at 25 °C for 2 h. The chain structure is illustrated in the inset (b) of Fig. 5. No bundled structures are observed. The global rotation motion of the chains of magnetic particles submitted to an oscillating magnetic field is measured using the light scattering technique. The sample is placed inside a temperature controlled cylinder and submitted to an oscillating magnetic field: two permanent magnets create a homogeneous static magnetic field of 0.2 T in the y direction and Helmholtz coils add a 150 mT magnetic field oscillating at ω in the perpendicular x direction. Consequently, the resulting field has an average value of approximately 0.2 T and oscillates within an 8° angle ($[-\beta_0; \beta_0]$), inducing oscillation of the chains of magnetic particles inside the tested sample. The beam of a He-Ne laser (L) operating at a wavelength of 632.8 nm runs through the sample (see Fig. 5). The light scattered by the sample then exhibits a diffusion streak that spatially oscillates in the direction perpendicular to the chains. A specific window has been designed to intercept the diffusion streak so that the intensity inside the window is directly proportional to the angle of the chains θ . The polar coordinates $r_+(\theta)$ and $r_-(\theta)$ of the window contours are

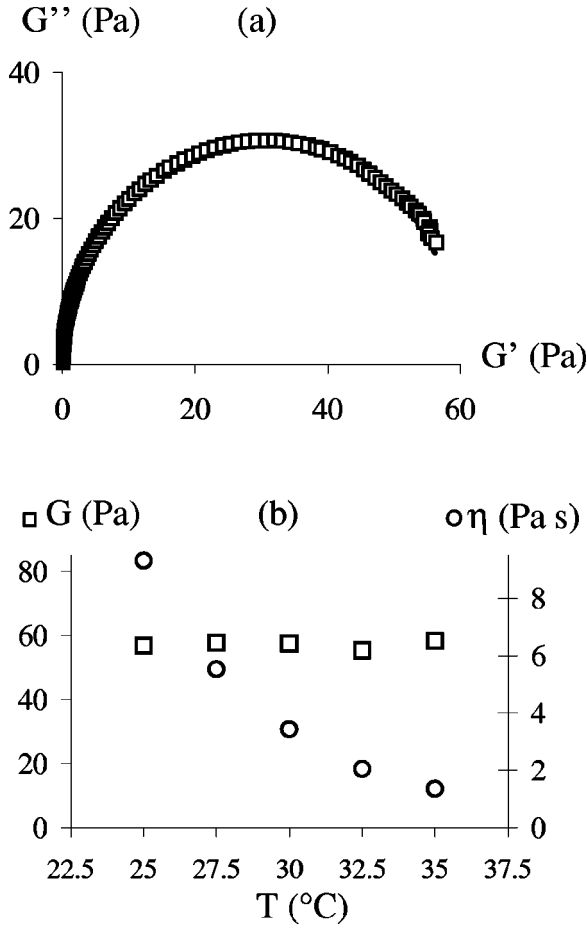


FIG. 4. (a) Cole-Cole plot of the viscoelastic modulus of an aqueous solution of $[CTAC]=0.1M$ with $[NaSal]=0.2M$ at $30^\circ C$ exhibiting a Maxwell type behavior (Couette rheometer measurements). (b) Temperature dependence of the shear modulus G and the viscosity η . η varies from 9.3 (25 °C) to 1.4 Pa s (35 °C) when temperature increases although G remains sensitively constant with a main value of 57 Pa.

given by the two equations $r_+ - r_- = k(\theta - \beta_0)$ and $r_+ + r_- = 2l$, where l is the distance between the window and the center of the laser beam and k is a proportionality constant, here chosen equal to l . The corresponding window is represented in the inset (a) of Fig. 5. The image of the window through a convergent lens is focused on a photodiode (PD). A lock-in amplifier extracts the phase and the magnitude of the ω component of the intensity detected by the photodetector. The time required to obtain the whole spectrum¹ (from 2 mHz to 100 Hz) attains 20 min and is small compared to the time required for the chains to form and lengthen (2 h). This allows us to consider the chains to be in a steady structure during the experiment. The intensity is also monitored on an oscilloscope. The linearity of the method was checked: the detected signal is sinusoidal, with

¹Points at 2, 5, 10, 25, and 50 mHz were obtained directly on the numeric oscilloscope during half a period, whereas the rest of the spectrum from 0.01 to 100 Hz was measured using the lock-in amplifier, 20 s per measurement.

very low harmonic content. By dividing the magnitude by its value for the lowest frequency (where no phase lag occurs), one obtains the magnitude and phase of θ_0/β_0 .

D. Optical microscopy

In order to visualize the rotation of a single chain of magnetic particles toward a permanent magnetic field, as described in Sec. II E, the magnetic setup presented in Fig. 6(a) has been adapted to a Leica inverted microscope. Two permanent magnets create a homogeneous field of 90 mT, generating the formation of chains in the field direction. At $t = 0$, a Helmholtz coil creates a 42 mT field in the orthogonal direction and one can observe the rotation of the chains rotate toward the 100 mT resulting field at 25° of the initial direction. The rotation of a single chain is observed through a $\times 100$ thermostated objective [see Fig. 6(b)] and recorded using video imaging.

IV. RESULTS

A. Oscillating chains

When submitted to a magnetic field rotating between the angles $-\beta_0$ and β_0 at frequency $\omega/2\pi$ [$\beta = \beta_0 \sin(\omega t)$], the chains of magnetic particles oscillate with the angle $\theta = \theta_0 \sin(\omega t + \varphi)$. Particles are inserted in the micellar solution described in Sec. II B and the phase φ and relative magnitude θ_0/β_0 are measured from 1 mHz to 100 Hz at 25, 27.5, 30, 32.5, and 35 °C. Four independent experiments were performed for each temperature to test the reproducibility of the assay, leading to an experimental error of 2% for the magnitude and 3.5% for the phase. The average points for each temperature are represented in Fig. 7. As predicted by the theory (Sec. I D), one can observe a minimum for the phase and an inflection point for the magnitude, at the same frequency ω_m . A non-negligible asymmetry appears, however, around ω_m , in contradiction to the theoretical curves shown in Fig. 2(b). This asymmetry is caused by the distribution of the chain length within the probed sample. Chains can indeed contain between two and 100 particles, the chain length ranging from 1 to about $60 \mu m$ [determined by observations through a microscope, illustrated in Fig. 5(a)]. The average chain length has been estimated at around $10 \mu m$ ($N = 20 \pm 10$), so that the parameter K defined by Eqs. (5), (7), and (9) has a mean value $K_m = (0.9 \pm 0.3) Pa^{-1}$. Equation (8) must then be weighted with the probability $P(K)$ reflecting the distribution of the parameter K , due to the distribution of the chain lengths:

$$\theta_0 = \beta_0 \int \frac{1 + i\omega\tau}{1 + i\omega\tau(1 + KG)} P(K) d(K). \quad (17)$$

A log-normal distribution [Fig. 8(a)] accurately models the experimental data:

$$P(K) = \frac{1}{(2\pi)^2 \sigma K} \exp\left[-\frac{1}{2\sigma^2} \left(\ln \frac{K}{K_0}\right)^2\right]. \quad (18)$$

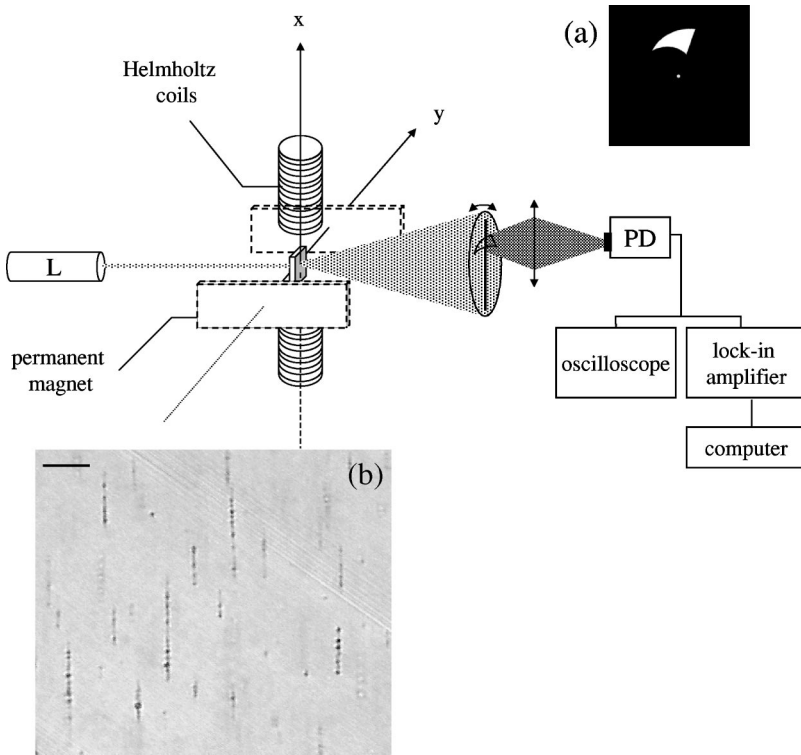


FIG. 5. Schematic diagram of the light scattering experimental setup. A 633 nm laser beam runs through the sample submitted to a spatially oscillating magnetic field. The intense scattered streak is perpendicular to the chains' direction and is intercepted by the window represented in inset (a) of the figure. Using a photodiode detection of the window image through a convergent lens, the angular magnitude and phase lag of the chains at the field frequency are extracted using a lock-in amplifier. The photodiode signal is also monitored on an oscilloscope. (b) Chains of magnetic particles of 650 nm diameter for a sample placed in a 0.2 T homogeneous field for 2 h observed in a microscope with magnification $\times 40$. Bar stands for 10 μm .

For all temperatures, Eqs. (17) and (18) with $\sigma=0.85$ and $K_0=0.6 \text{ Pa}^{-1}$ (corresponding to $K_m=0.9 \text{ Pa}^{-1}$) provide a good description (black lines in Fig. 7) of the experimental data. Determining the relaxation time τ through fitting is accurate and is plotted as a function of temperature in Fig. 8(b). The same relaxation times are obtained in macroscopic and

microscopic measurements, justifying *a posteriori* the hypothesis that the elastic and dissipative rotational factors κ_e and κ_v are equal. As the exact distribution of the number of particles per chain is not precisely known, this assay only gives an estimation of the shear modulus G , that is found not dependent on temperature, with a mean value $G=(75 \pm 25) \text{ Pa}$.

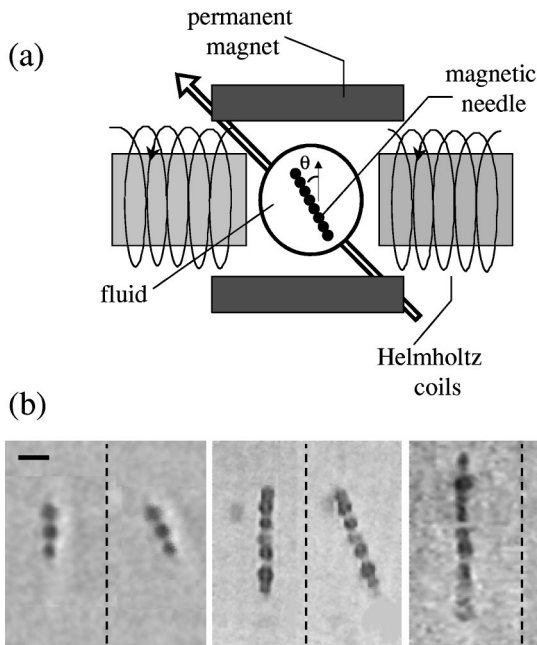


FIG. 6. (a) Sketch of the magnetic setup allowing microscope observation of the rotation of chains of magnetic particles toward a permanent magnetic field. (b) Images of the rotation of chains of particles through $\times 100$ magnification objective (from left to right, $N=3, 7, 10$). Bar stands for 1 μm .

B. Rotation toward a permanent magnetic field

To obtain an accurate evaluation of both viscous and elastic moduli, a second series of experiments is performed using the setup described in Sec. II D. Direct measurements of the chain length (or identically the number of particles within the considered chain) are performed under a microscope in order to access the factor K .

First, the rotation of chains of different lengths ($N=3,5,7,10,15$) toward an applied magnetic field is measured as a function of time for the micellar solution at 30 °C. Three independent measurements were achieved for each number N of particles per chain and the average curves are represented on Fig. 9(a). For $N=15$, we assume the Shish-Kebab model to be valid and Eq. (3) gives the value of the geometrical rotation factor: $\kappa(N=15)=223$. The parameter K is then equal to 1.3 Pa^{-1} [$\kappa_m(N=15)=169 \text{ Pa}$; see Eq. (7)] and a fit of the experimental data [black lines in Fig. 9(a)] using Eq. (15) gives the relaxation time $\tau=(0.06 \pm 0.002) \text{ s}$ and the shear modulus $G=(58 \pm 1) \text{ Pa}$. The parameter K for $N=3,5,7,10$ is then obtained through fitting the four other curves of Fig. 9(a) and the equivalent geometrical rotational factors κ are represented on Fig. 9(b) with respect to N . κ goes from the value corresponding to an ellipsoidal shape for small N to the value determined using the chain model for $N > 10$. The overall behavior is correctly represented by the

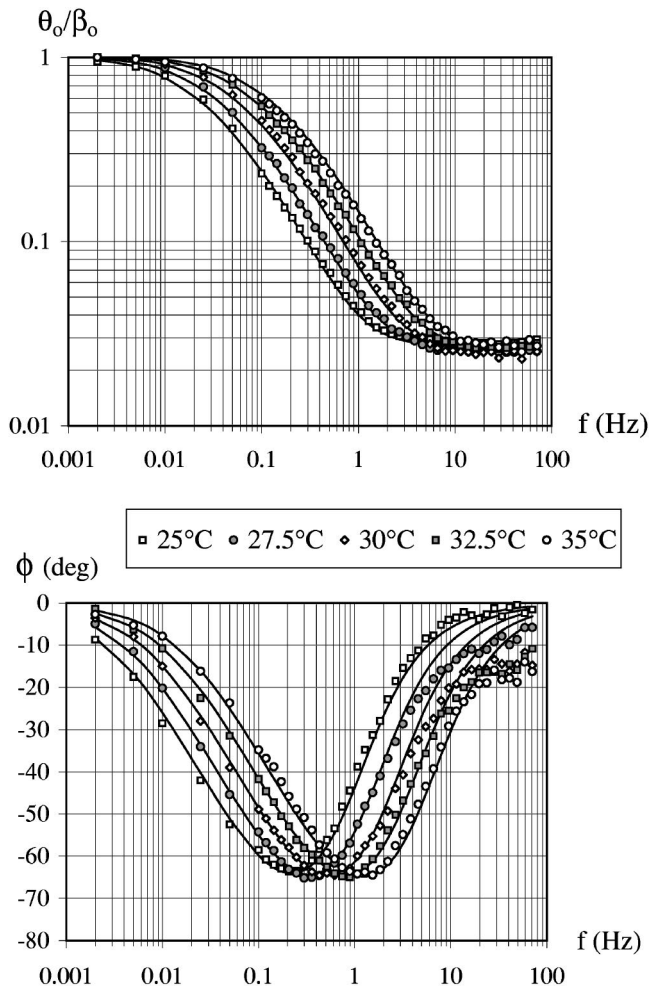


FIG. 7. Experimental Bode diagrams for the micellar solution at 25, 27.5, 30, 32.5, and 35 °C obtained by the light scattering assay. Experimental points are correctly fitted by Eqs. (17) and (18) (black lines).

phenomenological law described in Eq. (5) with $b=2.4$.

Secondly, the rotation of chains containing seven particles is measured for the five different temperatures. Each measurement is repeated three times. The average curves are represented on Fig. 10(a) with the fits obtained using Eqs. (12) and (13) (black lines in the figure). This method yields the same values of the relaxation times τ as the values obtained using the light scattering method. However, as the factor K can now be calculated using Eq. (5), the shear modulus G is precisely determined for each temperature. Finally, the shear modulus G and the viscosity η obtained by this microrheology assay are represented in Fig. 10(b) and are coherent with the values obtained using the classical rheometer.

V. DISCUSSION AND PERSPECTIVES

Micrometer-sized magnetic particles, dispersed into soft materials and submitted to a constant magnetic field, self-organize in chains. When submitted to an additional magnetic field in the perpendicular direction, these chains rotate, providing an efficient tool to probe the viscoelastic charac-

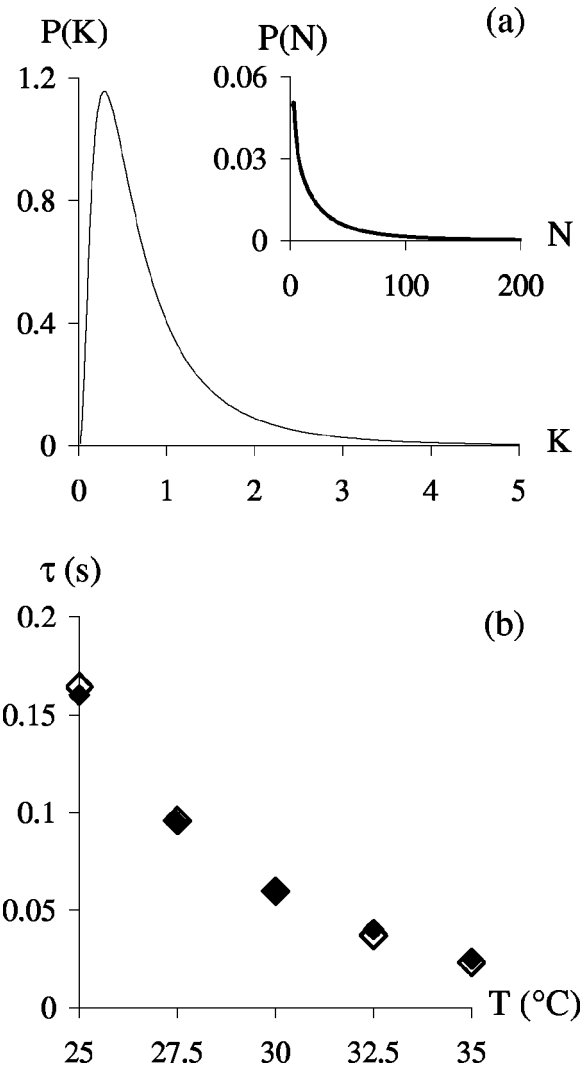


FIG. 8. (a) Log-normal distribution $P(K)$ of parameter K reflecting the distribution of the number of particles per chain within the tested solutions [corresponding distribution $P(N)$ shown in the inset]. (b) Temperature dependence of the relaxation time of the micellar solutions measured using light scattering (black diamonds) and by classical rheology (white diamonds). The two sets of values correspond well.

teristics of the fluid. Two different techniques are used; one is global and the other is local.

The analysis of the streak line diffraction pattern of a laser beam passing through the sample gives access to the instantaneous angular orientation of the chains. When an alternating additional magnetic field is applied, the frequency response of the angular amplitude of the oscillation of the chains provides an accurate estimation of the viscoelastic relaxation time. Using a homogeneous micellar solution having a rheological Maxwellian behavior, this measurement is shown to correspond very well with results obtained using classical rheometry. The resulting assumption that the hydrodynamic viscous volume and elastic volume displaced by the chain are equal therefore holds ($\kappa_e = \kappa_m$). One must address at this stage the issue of the range of material viscoelastic properties accessible using this technique. It appears intuitive

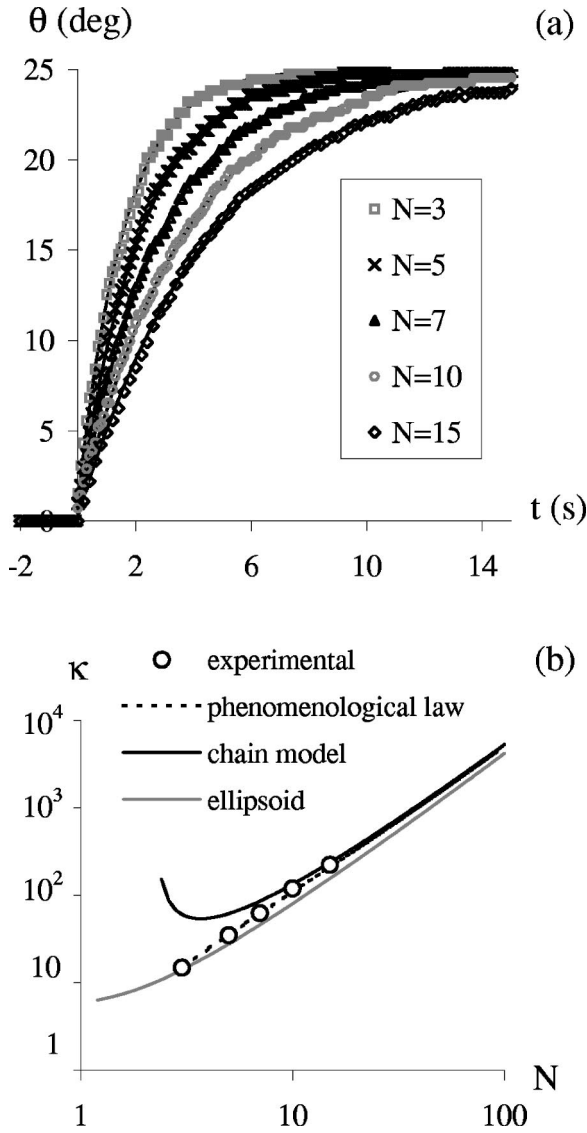


FIG. 9. (a) Experimental plots of the rotation angle at 30 °C of different chains ($N=3, 5, 7, 10,$ and 15) toward the applied 0.1 T magnetic field. Each curve is the average of three independent measurements. (b) Geometrical rotational factor κ as a function of N for an ellipsoidal probe (gray line, N is then assimilated to the aspect ratio of the ellipsoid) and a chain of N particles (Shish-Kebab model, black line). Experimental measurements are represented on the same plot (black circles) with the corresponding phenomenological law described in Eq. (5) (dashed line).

that the technique would not work in the highly dilute particle limit since the formation of the chains then requires an excessively long time and that one must also avoid too high a concentration of particles where aggregation of dipolar chains could occur. Let us estimate for a minimum volume fraction of 10^{-4} and a maximum one of 10^{-3} the range of viscoelasticities that can then be probed.

First, the formation of the chains themselves is crucial. The characteristic time for chain formation is given by

$$T_0 \sim \frac{\eta}{\mu_0 M_v^2} \phi^{-5/3}, \quad (19)$$

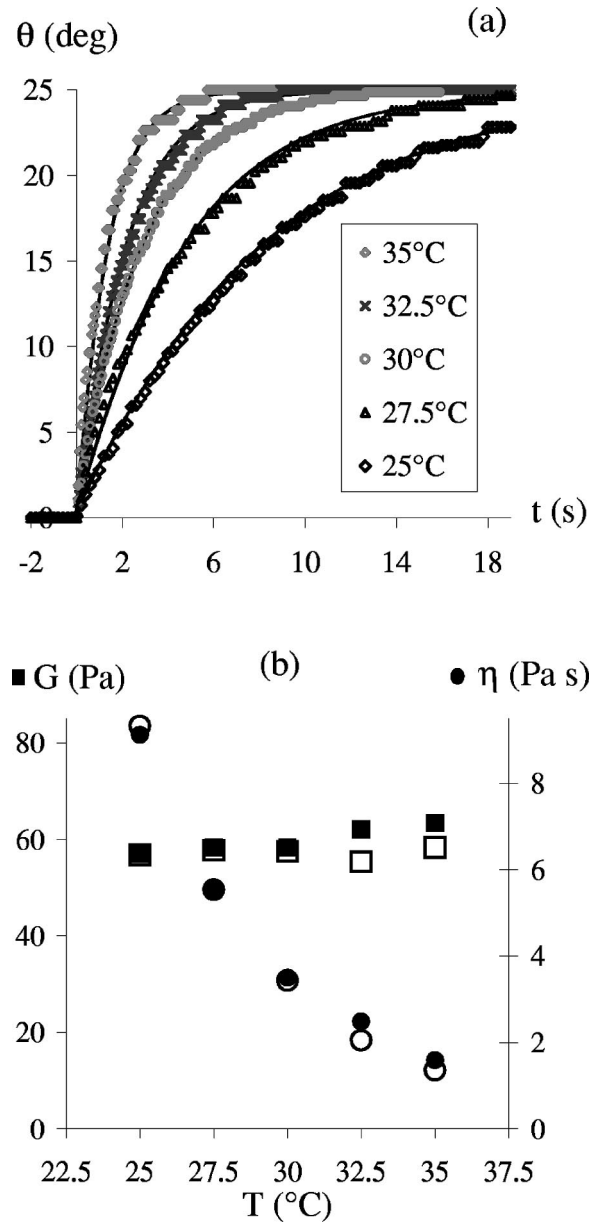


FIG. 10. (a) Experimental plots of the rotation angle as a function of time for a chain containing seven particles toward a permanent 0.1 T magnetic field in the micellar solutions at 25, 27.5, 30, 32.5, and 35 °C, the smaller the relaxation time (the higher the temperature), the faster the chain relaxes toward the applied field. Each curve is the average of three independent measurements. (b) Temperature dependence of the shear modulus G and the viscosity η . Black squares and circles are obtained by microscope microrheology measurement while white squares and circles are obtained by classical rheology experiment.

where η is the zero-frequency viscosity, ϕ is the volume fraction, and M is the particle volume magnetization. Numerical estimation for our experimental conditions [$M_v(B=0.2\text{ T})=10^4\text{ A m}^{-1}$, $\eta\sim 10\text{ Pa s}$ (chain formation at 25 °C), $\phi=5\times 10^{-4}$] leads to 3.5 h, in agreement with the observation that no aggregated chains are seen after the 2 h preparation of the sample under a magnetic field. This justifies also the assumption that no aggregation occurs during

the time required for the measure (20 min). Chain formation fails if the viscosity η is too large. The same happens if the particles are too dilute. Using our particles with a maximum volume fraction of 10^{-3} and considering that chain formation should not exceed 24 h, the largest viscosity that is accessible with our technique is $\eta_{\max} \sim 10^2$ Pa s. Conversely, if η is too small, the chain formation could be too fast for practical use. Using our particles with a minimum volume fraction of 10^{-4} , the lowest viscosity (corresponding to a characteristic time for chain formation of 1 h) that is accessible with our experimental conditions is $\eta_{\min} \sim 10^{-3}$ Pa s. Nevertheless, it is always possible to lower the limit of low viscosity by diminishing the magnetic field intensity.

Second, one must make sure that, once the chains are formed, the measurement is possible. In this way, on one hand, in order to be able to extract τ from the spectrum, it is necessary that KG is bounded between, say, 10^{-2} and 10^3 (this represents the dynamics given by the lock-in amplifier). Since $K \sim 1 \text{ Pa}^{-1}$ in our experimental conditions (mean number of 20 particles per chain), G must be bounded between 10^{-2} and 10^3 Pa. On the other hand, it is necessary to access about two decades around the minimum frequency, given in Eq. (14), with $K \sim 1 \text{ Pa}^{-1}$. Then, in order to neglect the chain formation during the course of the experiment (20 min), it is required that the period corresponding to the lower frequency used ($\omega_m/10$) is much smaller than T_0 . This condition directly leads to a minimum value of the shear modulus G_{\min} , satisfying $\sqrt{1+KG_{\min}}/KG_{\min} = \phi^{-5/3}/2\pi 10^2 \mu_0 M_v^2$, with $K \sim 1 \text{ Pa}^{-1}$. Finally, it is difficult to produce a magnetic field whose frequency exceeds 1 kHz. The higher frequency of the spectrum ($10\omega_m$) must therefore stay inferior to $f_{\max} = 1 \text{ kHz}$, providing a condition that both η and G must satisfy: $\eta \geq G/2\pi 10^3 \sqrt{1+KG}$, with $K \sim 1 \text{ Pa}^{-1}$. Figure 11 summarizes the accessible range for viscosity and elasticity using the presented rotational technique, for volume fractions in particles of 10^{-4} and 10^{-3} and for a volume magnetization of the particles $M_v = 10^4 \text{ A m}^{-1}$ (magnetic field applied 0.2 T).

The problems of chain aggregation and imprecise knowledge of chain lengths (which are mostly responsible for the limitations in the accessible viscoelasticities that can be probed) are overcome by using the direct observation of a single chain under a microscope. The relaxation of the chain toward a constant magnetic field is recorded on video. The chain structure is then precisely known in the particular region of interest and the angular response curves, the rotational analogs of compliance, are fitted using both elastic and viscous moduli as parameters. The geometrical factor κ involved in the theoretical description has been calibrated and

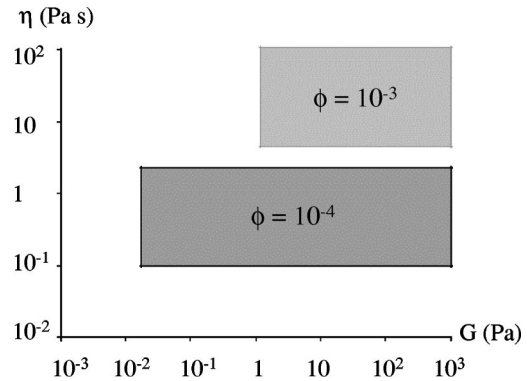


FIG. 11. Representation of the range of accessible viscoelasticities (in gray; viscosity η in Pa s and elasticity G in Pa) using the light diffusion technique, in our experimental conditions and for two different volume fractions ϕ of particles. One can also reduce the intensity of the applied magnetic field to probe lower viscosities.

found to be well described by the chain model for chains of aspect ratio larger than 10. The results match classical rheometry within 10%.

This simple and accurate microrheology technique using a rotational probe will be of major interest for viscoelastic measurements of biological semitransparent samples which are only available in small volumes (200 μl are sufficient). By varying the size of the probe (but not its aspect ratio), it will be possible to investigate how viscoelastic moduli of soft materials scale, therefore revealing the characteristic size of the mechanical structure of complex materials.

In the same way, the rheology of the cytoplasm of living cells may be investigated, using the local measurement of a single chain rotation in the cell interior. It has indeed been demonstrated [22] that magnetic nanoparticles are internalized within cells and concentrate inside intracellular endosomal compartments. Each magnetic endosome can be assimilated into a sphere of 0.6 μm and will be used as the equivalent therefore of the particles under consideration in this study. The magnetically induced rotation of these endosome chains will provide quantitative information about the local intracellular viscoelasticity.

ACKNOWLEDGMENTS

We would like to thank R. Vidal from the Merck Society for providing us with magnetic particles, Y. Raikher and F. Gazeau for fruitful discussions, and S. Williams for reading the manuscript. We are grateful to F. Elias for pertinent advice and a careful reading of the manuscript.

- [1] F. Ziemann, J. Radler, and E. Sackmann, *Biophys. J.* **66**, 2210 (1994).
 [2] F. Amblard, A. C. Maggs, B. Yurke, A. N. Pargellis, and S. Leibler, *Phys. Rev. Lett.* **77**, 4470 (1996).
 [3] A. R. Bausch, W. Moller, and E. Sackmann, *Biophys. J.* **79**,

720 (1999).

- [4] E. Helfer, S. Harlepp, L. Bourdieu, J. Robert, F. C. MacKintosh, and D. Chatenay, *Phys. Rev. Lett.* **85**, 457 (2000).
 [5] T. G. Mason and D. A. Weitz, *Phys. Rev. Lett.* **74**, 1250 (1995).

- [6] T. G. Mason, K. Ganesan, J. H. vanZanten, D. Wirtz, and S. C. Kuo, *Phys. Rev. Lett.* **79**, 3282 (1997).
- [7] F. Gittes, B. Schnurr, P. D. Olmsted, F. C. MacKintosh, and C. F. Schmidt, *Phys. Rev. Lett.* **79**, 3286 (1997).
- [8] B. Schnurr, F. Gittes, F. C. MacKintosh, and C. F. Schmidt, *Macromolecules* **30**, 7781 (1997).
- [9] M. Doi and S. F. Edwards, *The Theory of Polymer Dynamics* (Clarendon, Oxford, 1986).
- [10] F. Perrin, *J. Phys. Radium* **5**, 497 (1934); **7**, 1 (1936).
- [11] T. Gisler and D. A. Weitz, *Phys. Rev. Lett.* **82**, 1606 (1999).
- [12] G. Nisato, P. Hébraud, J.-P. Munch, and S. J. Candau, *Phys. Rev. E* **61**, 2879 (2000).
- [13] F. G. Schmidt, B. Hinner, and E. Sackmann, *Phys. Rev. E* **61**, 5646 (2000).
- [14] A. C. Maggs, *Phys. Rev. E* **57**, 2091 (1998).
- [15] Z. Cheng, P. M. Chaikin, and T. G. Mason, *Phys. Rev. Lett.* **89**, 108303 (2002).
- [16] G. Helgesen, P. Pieranski, and A. T. Skjeltorp, *Phys. Rev. Lett.* **64**, 1425 (1990).
- [17] S. Melle, G. Fuller, and M. A. Rubio, *Phys. Rev. E* **61**, 4111 (2000).
- [18] G. J. Besseres, I. F. Miller, and D. B. Yeates, *J. Rheol.* **43**, 591 (1999).
- [19] C. Wilhelm, F. Elias, J. Browaeys, A. Ponton, and J.-C. Bacri, *Phys. Rev. E* **66**, 021502 (2002).
- [20] L. Landau and E. Lifchitz, *Fluid Mechanics* (Pergamon, London, 1971).
- [21] V. M. Laurent, S. Hénon, E. Planus, R. Fodil, M. Balland, D. Isabey, and F. Gallet, *J. Biomech. Eng.* **124**, 408 (2002).
- [22] C. Wilhelm, F. Gazeau, J. Roger, J. N. Pons, and J.-C. Bacri, *Langmuir* **18**, 8148 (2002).